ACS OMEGA

http://pubs.acs.org/journal/acsodf

Article

Selective Determination of Norfloxacin in Pharmaceutical Formulations and Human Urine Samples Using Poly(8-aminonaphthaline-2-sulfonic Acid)-Modified Glassy Carbon Electrodes

Ameha Debalkie, Atnafu Guadie, Adane Kassa,* and Molla Tefera*

Cite This: *ACS Omega* 2023, 8, 25758−25765

Read Online

ACCESS | Metrics & More | Article Recommendations | Supporting Information

ABSTRACT: In this study, a glassy carbon electrode was modified potentiodynamically with poly(8-aminonaphthaline-2-sulfonic acid) [poly(ANSA)/GCE] for the detection of norfloxacin (NFN) in tablet formulations and human urine samples. Improvement of the effective surface area of the modified electrode and decreased charge-transfer resistance confirmed surface modification of the GCE by a conductive poly(ANSA) film. The appearance of an oxidative peak without a reductive peak in the reverse scan direction showed the irreversibility of the electrochemical oxidation of NFN in both the bare GCE and poly(ANSA)/GCE. A better coefficient of determination for the peak current on the square root of the scan rate (R^2 = 0.99514) than the scan rate (R^2 = 0.97109), indicating the oxidation of NFN at the poly(ANSA)/GCE, was predominantly diffusion mass transport-controlled. Under optimized pH and square wave parameters, the voltammetric current response of NFN at the poly(ANSA)/GCE showed linear dependence on the concentration, ranging from 1.0×10^{-8} to 4.0×10^{-4} M with a limit of detection of 4.1×10^{-10}. The NFN level in the studied tablet brands was in the range of 90.30−103.3% of their labeled values. Recovery results in tablet and urine samples ranged from 98.35 to 101.20% and 97.75 to 99.60%, respectively, and interference recovery results were less than 2.13% error in the presence of ampicillin, chloroquine phosphate, and cloxacillin. The present method had a better performance for the determination of NFN in tablet formulations and urine samples as compared with recently reported voltammetric methods due to its requirement of a simple electrode modification step, which provides the least limit of detection and a reasonably wider linear dynamic range.

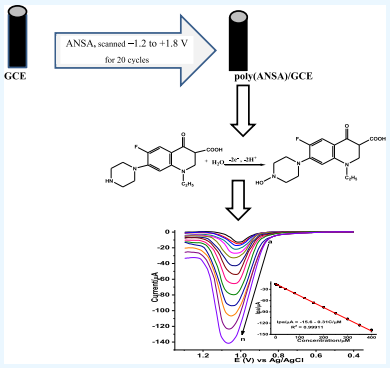

1. INTRODUCTION

An antibiotic is a chemotherapeutic agent that inhibits or stops the growth of microorganisms, such as bacteria, fungi, or protozoa. Antibiotics are classified by their chemical structure or the mechanism of action and are grouped into categories that include β-lactams, quinolones, tetracyclines, macrolides, and sulfonamides.[1] These quinolones are effective against Gram-positive and Gram-negative bacteria through inhibition of their DNA gyrase, a critical enzyme for bacterial chromosome replication.[2]

Norfloxacin [1-ethyl-6-fluoro-1,4-dihydro-4-oxo-7-(1-piperazinyl)-3-quinolone carboxylic acid] (Scheme 1) belongs to the fluoroquinolones family used against several types of bacteria and has been applied to veterinary and human medicine[3] to treat gastrointestinal, urinary, respiratory tract, ocular, and skin infections. Norfloxacin (NFN) is also used in patients with intra-abdominal infections in combination with antianaerobic agents.[4] Improper usage of NFN causes several side effects such as headache, depression, dizziness, nausea, and vomiting.[5] Since NFN is the most important antibiotic for bacterial infections, its accurate and precise determination is crucial.

Scheme 1. Structural Formula of Norfloxacin

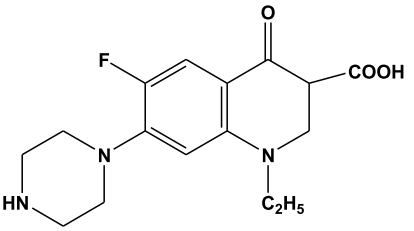

Spectrophotometry,[6−8] chromatography,[9,10] and chemiluminescence[11] are among the techniques reported for NFN determination in different real samples. However, these techniques require large amounts of organic solvents, expensive

Received: February 7, 2023
Accepted: June 26, 2023
Published: July 10, 2023

instrumentation, a long analysis time, complex sample pretreatments, and are non-eco-friendly.[12,13] In this regard, electrochemical methods, including, voltammetry are accurate, reproducible, fast, environmentally friendly, and often selective methods.[12−16]

Attempts have been made on the electrochemical determination of NFN in different real samples using modified electrodes, including MWCNT-CPE/prGO-ANSA/Au,[12] Ni/NiO/C/β-CD/RGO/GCE,[14] MWCNT/Nafion/GCE,[17] EPPGS,[3] CuO/MWCNT/GCE,[18] and poly(methyl red)/GCE.[19] Most of these reported sensors required expensive modifiers like rGO and Au nanoparticles with complex preparation procedures. In this regard, we reported a poly(8-aminonaphthaline-2-sulfonic acid)-modified glassy carbon electrode [poly(ANSA)/GCE] for the electrochemical determination of NFN in tablet formulations and human urine samples. To date, an electrochemical method based on poly(ANSA)/GCE fabricated from easily available material, has not been reported for the determination of NFN.

2. MATERIALS AND METHODS

2.1. Chemicals and Apparatus. All chemicals are of analytical grade, used without further purification. Norfloxacin (≥99.0%, Sigma-Aldrich), 8-aminonaphthaline-2-sulfonic acid (≥98.0%, Blulux Laboratories Pvt. Ltd.), $K_3[Fe(CN)_6]$ and $K_4[Fe(CN)_6]$ (98.0% HDH laboratory samples, England), potassium chloride (99.5%, Blulux Laboratories Pvt. Ltd.), sodium monohydrogen phosphate and sodium dihydrogen phosphate (≥98.0%, Blulux Laboratories Pvt. Ltd.), hydrochloric acid (37%, Fisher Scientific), sodium hydroxide (Extra Pure, lab tech chemicals), and nitric acid (70%, Fisher Scientific).

CHI 760E electrochemical workstation (Austin, Texas, USA), pH meter (Adwa, AD 8000, pH/mv/EC/TDS), electronic balance (Nimbus, ADAM Equipment, USA), refrigerator (Lec Refrigeration PLC, England), and deionizer (Evoqua Water Technologies) were also used throughout the experiment.

2.2. Electrochemical Measurements. Electroanalytical measurements were performed using a conventional three-electrode system consisting of Ag/AgCl (3.0 M KCl) as a reference electrode, Pt coil as a counter electrode, and an unmodified GCE (3 mm diameter) or the poly(ANSA)/GCE as a working electrode. EIS and CV techniques were used to characterize the modified electrode and/or to investigate the electrochemical behavior of NFN at the surface of the poly(ANSA)/GCE at various scan rates and pH values. Square wave voltammetry (SWV) was employed for the quantitative determination of NFN in three tablet brands and human urine samples.

2.3. Procedures. *2.3.1. Preparation of Poly(ANSA)/GCE.* A mirror finish polished GCE was immersed in 0.1 M phosphate buffer solution (PBS) of pH = 7.0 containing 2.0 mM ANSA and scanned between an optimized potential window (−1.2 to+1.8 V) for 15 cycles at a scan rate of 100 mV s^{-1}. The poly(ANSA)/GCE was rinsed with deionized water and stabilized in 0.5 M H_2SO_4 with a potential window of −0.80 and +0.80 V until a steady cyclic voltammogram was obtained. Finally, the modified electrode was dried in the air and used for further experiments.

2.3.2. Preparation of Standard NFN Solutions. A stock solution of 5.0 mM standard NFN solutions was prepared by dissolving 159.6 mg of NFN in 100 mL of deionized water. Working standard solutions of NFN were prepared from the stock solution by serial dilution with PBS at the required pH values.

2.3.3. Pharmaceutical Tablet Sample Preparation. For real sample analysis, available commercial brands of NFN tablets (Medochemie Ltd., pharmaceutical company, Cyprus; East African pharmaceutical PLC (EAP), Ethiopia; and Sansheng Pharmaceutical PLC (SSP), China) with average tablet mass of 542.2, 683.2, and 590.0 mg/tablet were obtained from a local drug store in Bahir Dar, Ethiopia. Five tablets of each brand were completely ground and homogenized using a mortar and pestle. 2.0 mM tablet sample stock solutions for each tablet brand were prepared by transferring a mass equivalent to 63.9 mg (87.57, 109.14, and 94.3 mg, respectively) NFN tablet powder to a 100 mL volumetric flask and filled up to the mark with deionized water. Furthermore, working tablet sample solutions in pH = 7.5 PBS for each tablet brand were prepared from the respective tablet stock solution through serial dilution.

3. RESULTS AND DISCUSSION

3.1. Fabrication of Poly(ANSA)/GCE. In the attempt to deposit the poly(ANSA) film on the surface of GCE potentiodynamically, the number of scan cycles and potential scan windows were the most important parameters to be optimized, followed by the film thickness. Figure S1A shows the current response of the poly(ANSA)/GCE for NFN as a function of the potential window (between −0.4 and +1.8, −0.8 and +1.8, −1.4 and +1.8, and −1.2 and +1.8 V). As can be seen from the inset of the figure, the poly(ANSA)/GCE fabricated in the potential window between −1.2 and +1.8 V showed the highest catalytic effect toward oxidation of NFN (curve d of Figure S1A).

In this study, the number of scan cycles in the range of 10−30 was investigated to control the film thickness (Figure S1B). As can be observed from the inset of the figure, the anodic peak current of NFN increased with the number of scan cycles, although with differing slope (inset of Figure S1B). As a compromise between the current and over potential advantages and increased analysis cost, 15 scan cycles were taken as the optimum number of scan cycles. Hence, the poly(ANSA)/GCE synthesized from ANSA in pH 7.0 PBS scanned between −1.2 and +1.8 V for 15 cycles (Figure 1) was selected for determination of NFN in tablet formulation and human urine samples.

As shown in Figure 1, anodic peaks (a, b, and c) and cathodic peaks (a′ and b′) were observed whose current response increased with increasing scan cycles, indicating the growth of the electroactive polymeric film at the electrode surface. As shown clearly in the figure, the voltammogram of the poly(ANSA)/GCE displayed distinct redox peaks (inset B of Figure 1) which are not exhibited at the GCE, confirming the immobilization of the electroactive poly(ANSA) film at the surface of the GCE.

3.2. Electrochemical Characterization of Poly(ANSA)/GCE. *3.2.1. Characterization by Cyclic Voltammetry.* Cyclic voltammetry (CV) was used to follow the deposition of the polymer film on the surface of the GCE. The cyclic voltammetric response for $Fe(CN)_6^{3-/4-}$ at unmodified and modified forms of GCEs are displayed in Figure 2. Pair of characteristic redox peaks of $Fe(CN)_6^{3-/4-}$ appeared at the studied electrodes although with differing current intensities and peak to peak separation.

https://doi.org/10.1021/acsomega.3c00805
ACS Omega 2023, 8, 25758−25765

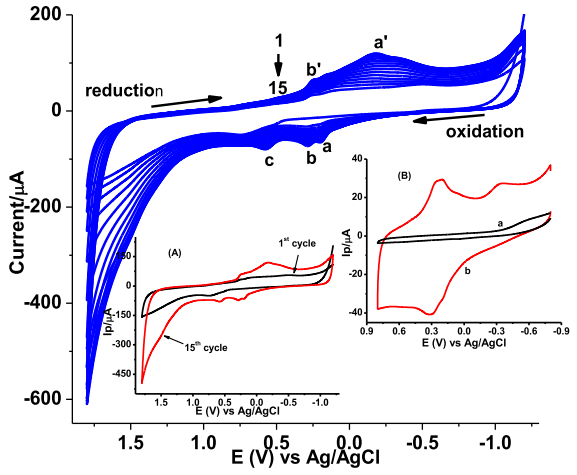

Figure 1. Repetitive CVs of the GCE in pH 7.0 PBS containing 2.0 mM ANSA scanned between −1.2 and +1.8 V at a scan rate of 100 mV s^{-1} for 15 cycles. Inset: (A) 1st cycle and 15th cycle CVs and (B) CVs of the (b) bare GCE and (b) stabilized poly(ANSA)/GCE in monomer free 0.5 M H_2SO_4.

In contrast to the bare GCE, a pair of peaks with comparably improved current intensity and peak-to-peak potential separation was observed at the poly(ANSA)/GCE. The peak potential separation (ΔE_p) is significantly reduced from 415 mV at the GCE to 85 mV at the poly(ANSA)/GCE, mainly associated with increasing conductivity of the surface material. The peak current intensity enhancement could be ascribed to the increased effective surface area and/or affinity of the electrode surface for the analyte.

The active surface area of the working electrode was estimated from the slope values of the plot of I_{pa} *versus* $\nu^{1/2}$ of each electrode on $Fe(CN)_6^{3-/4-}$ (Figure S2) using the Randles−Sevcik equation eq 1.[20]

$$I_{pa} = 2.69 \times 10^5 n^{3/2} A D^{1/2} \nu^{1/2} C_o \quad (1)$$

where I_{pa} is the anodic peak current, n is the number of electron transfer, A is the active surface area of the electrode, D is the diffusion coefficient, Co is the concentration of the probe, and ν is the scan rate.

The surface areas of both electrodes were calculated based on the Randles−Sevcik equation and it was found that the surface area of the poly(ANSA)/GCE (0.184 cm^2) was 3.4 times larger than that of the bare GCE (0.054 cm^2) (Figure S2A,B), indicating that the electrochemical activity for the redox probe is enhanced on the poly(ANSA)modified electrode surface.

3.2.2. Electrochemical Impedance Spectroscopic Characterization. Electrochemical impedance spectroscopy (EIS) is a promising technique to understand the electrochemical properties of the electrode surface, and the interface between the surface of the modified electrode and analyte,[21] was used to investigate the electrode modification and evaluate the electron conductivity of the material with which the GCE was modified. EIS spectra of both the bare GCE (curve a) and the modified GCE (curve b) in pH 7.0 PBS containing 10.0 mM of $[Fe(CN)_6]^{3-/4-}$ and 0.1 M of KCl are shown in Figure 2B. As shown in the figure, the semicircles at the high-frequency region with varying diameters are attributed to the charge-transfer resistance (R_{ct}) and at the semicircles at low-frequency region represent the diffusion of the $[Fe(CN)_6]^{3-/4-}$ from the bulk to the solution−electrode interface.

Summary of circuit elements including solution resistance (R_s), R_{ct}, and double layer capacitance (C_{dl}) for both bare and poly(ANSA)/GCEs as estimated from the corresponding Nyquist plot using eq 2[20]

$$C_{dI} = \frac{1}{2\pi R_{ct} f} \quad (2)$$

where C_{dI} is the double layer capacitance, f is the frequency corresponding to the maximum imaginary impedance (reactance) value on the Nyquist plot, and R_{ct} is the charge-transfer resistance.

The R_{ct} value for the poly(ANSA)/GCE (375 Ω, curve b) was much lower than the unmodified GCE (5427 Ω, curve a), demonstrating that the ANSA film on the GCE surface greatly enhanced the conductivity and hence the electron-transfer rate between the substrate and the analyte, which could be attributed to the conductive nature of the polymer film.

3.3. Cyclic Voltammetric Investigation of NFN. *3.3.1. Electrochemical Behavior of NFN at the Poly(ANSA)/GCE.* Enhanced effective surface area and low R_{ct} values of the

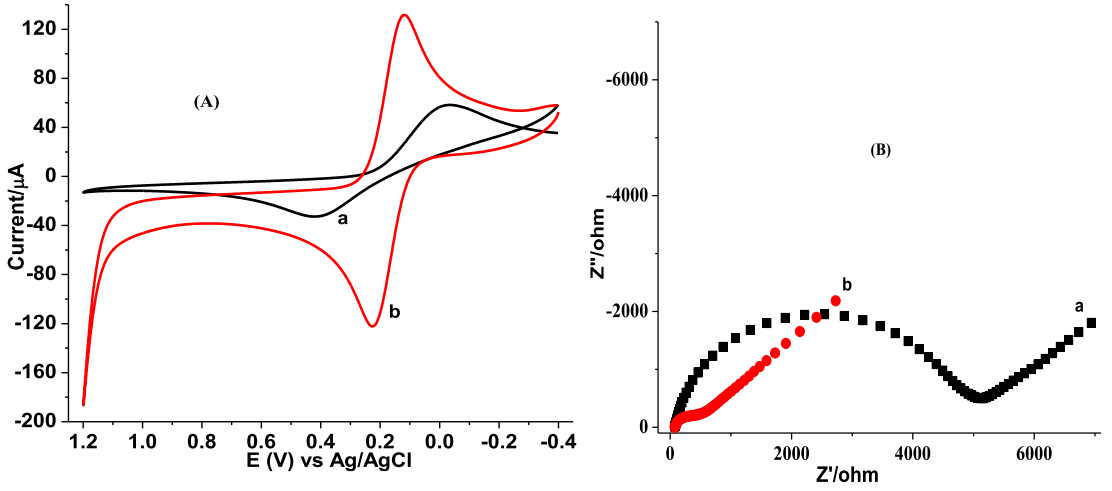

Figure 2. A) CV curves and (B) Nyquist plots of the (a) bare GCE and (b) poly(ANSA)/GCE in pH 7.0 PBS containing 10.0 mM $[Fe(CN)6]^{3-/4-}$ in 0.1 M KCl at a scan rate of 100 mV s^{-1} in the frequency range: 0.01−100,000 Hz, amplitude: 0.01 V, and potential: 0.23 V.

https://doi.org/10.1021/acsomega.3c00805
ACS Omega 2023, 8, 25758−25765

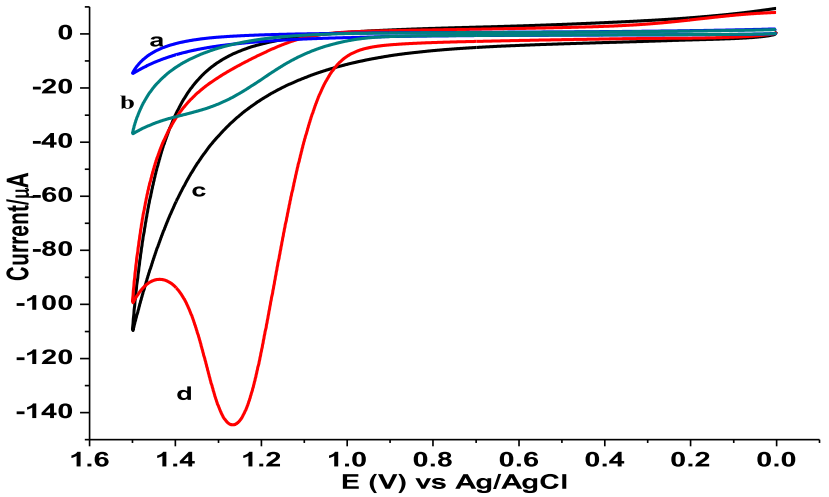

Figure 3. CV curves of the bare GCE (a,b) and poly(ANSA)/GCE (c,d) in the absence (a,c) and presence (b,d) of 1.0 mM NFN in pH 7.0 PBS at a scan rate of 100 mV s^{-1}.

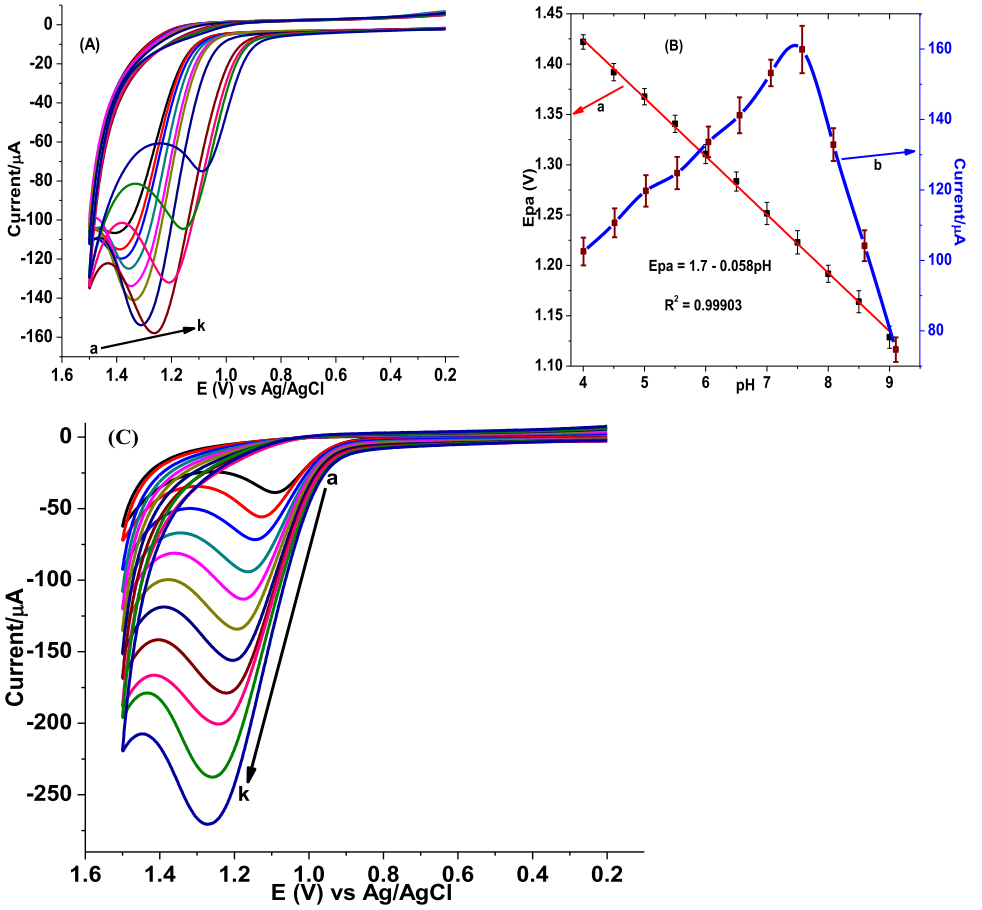

Figure 4. (A) CV curves of the poly(ANSA)/GCE in PBS of various pH values (a−k: 4.0, 4.5, 5.0, 5.5, 6.0, 6.5, 7.0, 7.5, 8.0, 8.5, and 9.0, respectively) containing 1.0 mM NFN, (B) plot of the peak (a) potential and (b) current *versus* pH values, and (C) effect of scan rates (a−k: 10, 20, 40, 60, 80, 100, 125, 150, 200, 250, and 300 mV s^{-1}, respectively) on peak current of 1.0 mM NFN in pH 7.5 PBS.

poly(ANSA)/GCE are excellent indicators of the catalytic activity of an electrode surface toward NFN oxidation. The electrochemical behavior of 1.0 mM NFN in pH 7.0 PBS at the poly(ANSA)/GCE and GCE was studied (Figure 3).

In contrast to the shorter and broader oxidative peak about 1.37 V at the GCE (curve a of inset), appearance of a well-defined oxidative peak at a potential of 1.25 V with five folds of current enhancement at the poly(ANSA)/GCE (curve b of the inset) indicated the catalytic effect of the poly(ANSA) film toward the oxidation of NFN. The remarkable signal enhancement at the poly(ANSA)/GCE as compared to the bare electrode might be due to the strong interaction of NFN with the poly(ANSA)/GCE *via* hydrogen bonding between the amine ($-NH_2$) and carboxylic (−COOH) groups of the

https://doi.org/10.1021/acsomega.3c00805
ACS Omega 2023, 8, 25758−25765

Scheme 2. Proposed Oxidation Mechanism of NFN

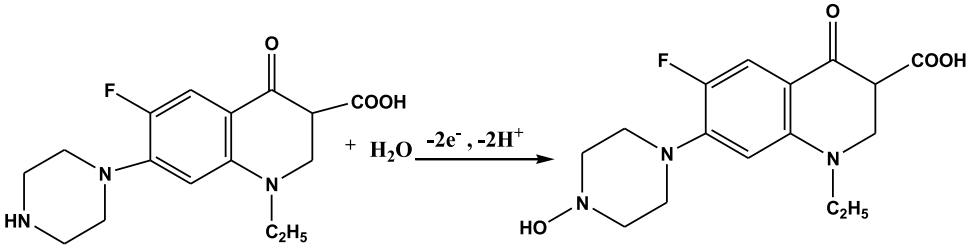

analyte with amine ($-NH_2$) and sulfonic groups (HSO_4) of the polymer. Besides, the $\pi-\pi$ interaction between NFN and the polymer attributes the strong coupling that could enhance the reaction rate.[22,23]

3.3.2. Effect of Supporting Electrolytes. Besides the nature of the electrode, the type of supporting electrolytes and pH also usually determine the electrochemical behavior of electroactive species. The common types of supporting electrolytes, phosphate buffer solution (PBS), acetate buffer solution (AB), and Britton−Robinson buffer solution (BR), which all exhibit buffering capacity at pH = 5.0,[15] were considered in this study. The cyclic voltammograms of 1.0 mM NFN in pH = 5.0 of the three buffer solutions at the poly(ANSA)/GCE are presented in Figure S3. The oxidation of NFN at the poly(ANSA)/GCE occurred almost at the same peak potential for both supporting electrolytes. However, NFN has provided the highest peak current in PBS supporting electrolyte compared with AB and RB electrolytes, therefore, PBS is the best of the studied electrolyte solutions. Therefore, PBS prepared by mixing equimolar amount (0.1 M) of NaH_2PO_4 and Na_2HPO_4 was used as a supporting electrolyte in this study.

3.3.3. Effect of pH and Scan Rates. To determine whether a proton has taken part in the reaction, evaluate the proton-to-electron ratio, and explain the type of interaction between the analyte and electrode surface, an investigation of the pH effect on peak current and peak potential of electroactive species at an electrode was crucial. Therefore, the effect of pH on NFN at the poly(ANSA)/GCE was investigated in the range of 4.0−9.0 using CV (Figure 4A). The observed peak potential shift in the negative direction in the studied pH range and indicated proton participation during the oxidation of NFN at the poly(ANSA)/GCE, with a slope of 0.058 V for the plot of E_{pa} *versus* pH of the PBS (curve a of Figure 4B) showing the involvement of equal protons and electrons (1:1).[12,13] Moreover, the peak current of NFN at the poly(ANSA)/GCE increased as pH values increased from pH 4.0 to 7.5, which then decreased at pH values beyond 7.5 (curve b of Figure 4B), making pH = 7.5 the optimum.

Hence, a reaction mechanism involving two electrons and two protons was proposed (Scheme 2), which is in agreement with the mechanism previously reported in the literature[17] for NFN oxidation at the poly(ANSA)/GCE.

The influence of the scan rate on the peak potential and peak current was studied in order to show the irreversibility of NFN oxidation and to investigate the rate-determining step during the reaction of NFN at the poly(ANSA)/GCE. Figure 4C describes the cyclic voltammograms of 1.0 mM NFN in pH 7.5 PBS at a scan rate in the range of 10−300 mV s^{-1}. The anodic peak potential of NFN shifted with increasing scan rate and confirmed the irreversibility of NFN oxidation.

A lower coefficient of determination (R^2 = 0.97109) for the dependence of NFN oxidative peak current on the scan rate than on the square root of the scan rate (R^2 = 0.99514) indicated that the oxidation reaction of NFN at the poly(ANSA)/GCE was predominantly controlled by diffusion mass transport.[14−17] This was further confirmed by the slope value of 0.59 for the plot of log (peak current) *versus* log (scan rate) (Figure S4), which is in agreement with the value of 0.50 for an ideal diffusion-controlled reaction.[20]

The number of electrons involved during oxidation of NFN at the poly(ANSA)/GCE was determined from cyclic voltammetric data. For an irreversible process, the value of αn was determined by the difference between the peak potential (E_p) and the half-wave potential ($E_{1/2}$), employing eq 3[20]

$$E_p - E_{1/2} = 47.7/\alpha n \tag{3}$$

where α is the charge-transfer coefficient and n is the number of electrons transferred.

Taking E_p and $E_{p1/2}$ for the cyclic voltammogram at a scan rate of 100 mV s^{-1} to be 1169 and 1112 mV, respectively, the value of αn was calculated to be 0.84.

The relationship between E_p and $\ln\nu$ for an irreversible process obeys eq 4[20]

$$E_p = E^\circ + \frac{RT}{(1-\alpha)nF}\left\{0.780 + \ln\left(\frac{D_R^{1/2}}{k^\circ}\right) + \ln\left[\frac{(1-\alpha)nF\nu}{RT}\right]^{1/2}\right\} \tag{4}$$

where E_p is the peak potential, E° is the formal potential, α is the electron-transfer coefficient, k^0 (s^{-1}) is the electrochemical rate constant, and the other parameters with their usual meanings.

From the slope value (slope = $\frac{RT}{2(1-\alpha)nF}$ = 0.019) for the fitted line [E_{pa} (V) = 0.96 + 0.019 ln ν] of the curve of plot of E_p *versus* ln (scan rate) (Figure S4D), the value of $n(1-\alpha)$ at the experimental temperature of 25 °C calculated using eq 4 was 0.67. Based on the values of αn obtained from eq 3 and $n(1-\alpha)$ from eq 4, the value n was calculated as 1.51(~2), *i.e*, the oxidation of NFN was carried out by the transfer of two electrons. For a two-electron oxidation of NFN, the value of α was estimated to be 0.66, confirming the irreversibility of the oxidation of NFN at the surface of the poly(ANSA)/GCE.

3.4. SWV Investigation of NFN at the Poly(ANSA)/GCE. Due to the ability of SWV to discriminate Faradaic current from non-Faradaic current than cyclic voltammetry,[15] it was selected for the quantification of NFN in pharmaceutical tablet formulations and human urine samples. Figure 5 shows SWVs of 1.0 mM NFN in pH 7.5 PBS at the bare GCE and

https://doi.org/10.1021/acsomega.3c00805
ACS Omega 2023, 8, 25758−25765

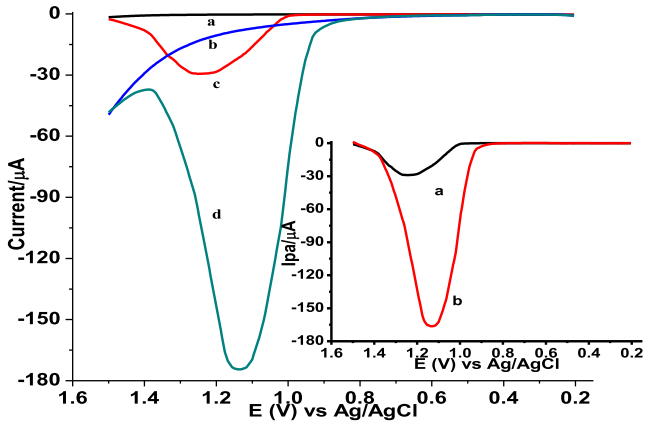

Figure 5. SWVs of the GCE (a, c), and poly(ANSA)/GCE (b,d) in PBS pH 7.5 containing no NFN (a,b) and 1.0 mM NFN (c,d) at step potential: 4 mV, amplitude: 25 mV, and frequency: 15 Hz. Inset: blank subtracted SWVs of (a) unmodified and (b) poly(ANSA)/GCE.

poly(ANSA)/GCE. A well-shaped oxidative peak with about six folds of current at much reduced potential at the poly(ANSA)/GCE (curve b of inset) compared with the oxidative peak at the GCE (curve a of the inset) signified the catalytic role of the poly(ANSA) film toward the oxidation of NFN.

For further analysis, selected SWV parameters (step potential, amplitude, and frequency) were optimized. Although the increase in peak current with increasing SWV parameters is implicit, these parameters were optimized by making a compromise between the increased Faradic peak current and the accompanied capacitive current (Figure S5). Hence, 6 mV,35 mV, and 20 Hz were chosen as the optimum step potential, amplitude, and frequency, respectively.

3.5. Calibration Curve. Figure 6 presents the background corrected SWVs of different concentrations of NFN at pH 7.5 PBS at the poly(ANSA)/GCE. Under the optimized solution and method parameters, the peak current of NFN at the poly(ANSA)/GCE is linearly proportional to the NFN concentration in the range of 0.01−400 μM (inset of Figure 6) with a limit of detection (LoD) (3 s/m, s is the standard deviation of the blank and m is the slope of calibration curve for n = 7) and a limit of quantification (10 s/m) of 0.41 and 1.36 nM, respectively. The low associated % RSD values (below 3.5% for n = 3) showed the accuracy and precision and hence validated the applicability of the developed method based on electrode modifiers for the determination of NFN.

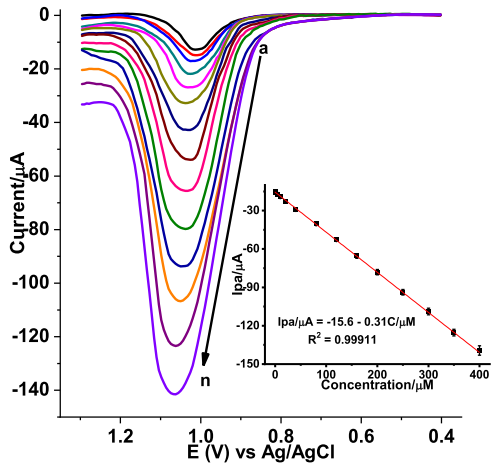

Figure 6. Background corrected SWVs of the poly(ANSA)/GCE in pH 7.5 PBS containing various concentrations of NFN (a−n: 0.01, 0.1, 1.0, 10.0, 20.0, 40.0, 80.0, 120.0, 160.0, 200.0, 250.0, 300.0, 350.0, and 400.0 μM, respectively) at E_{step} 6 mV, E_{amp} 35 mV, and frequency 20 Hz. Inset: plot of I_{pa} (% RSD as error bar) *vs* concentration of NFN.

3.6. SWV Determination of NFN in Real Samples Using the Poly(ANSA)/GCE. *3.6.1. Pharmaceutical Tablet Samples.* The level of NFN in three brand NFN tablet samples was determined using the developed sensor, and the detected content was further compared with the nominal NFN amount of the tablet powder portion according to the tablet label. The SWV curves for 20.0 and 40.0 μM nominal NFN for each tablet brand were recorded (Figure S6). The detected NFN content of each tablet brand calculated from the calibration regression equation was compared with the nominal NFN content of the company's label (Table 1).

Table 1. Summary of Detected NFN Content and Percent Detected as Compared to the Nominal Value for Each Analyzed Tablet Brand

tablet brand	labeled amount (μM)	detected amount (μM)	detected NFN (%)
CSPC	20.0	18.87 ± 0.023	94.35
	40.0	39.03 ± 0.014	97.57
SSP	20.0	20.65 ± 0.025	103.25
	40.0	40.64 ± 0.016	101.66
EAP	20.0	18.06 ± 0.020	90.30
	40.0	38.06 ± 0.015	95.15

As can be seen from the table, the detected NFN content ranged between 90.3 and 103.3% of what was expected with a % RSD value under 0.12% (n = 3). In contrast to the expected level of NFN in the three studied tablet brands, observed slight variations may be accounted for by experimental errors like possible mass loss during preparation, degradation during storage, or company error during preparation.

3.6.2. Human Urine Sample. The absence of an observable peak at the characteristic oxidation potential of NFN (curve a of Figure S7a) indicates the absence of NFN in the analyzed human urine sample; the reliability was examined by spike recovery analysis. The appearance of a peak (Figure S7a) at a potential away from that of NFN assigned peak-A for uric acid and peak-B for creatinine.[24]

3.7. Validation of the Proposed Method. *3.7.1. Spiked Recovery Study.* Recovery studies were carried out by spiking tablets and human urine samples with a standard solution of NFN using SWV the poly(ANSA)/GCE.[25]

3.7.1.1. Urine Samples. Human urine samples were spiked with 20.0, 40.0, and 80.0 μM NFN (Figure S7) and the SWV of urine samples showed a peak for uric acid at 0.2 V and creatinine at 0.6 V, both with exactly constant current intensity regardless of the level of spiked NFN. However, the appearance of a peak (peak C) at the characteristic oxidation potential of NFN whose peak current increased with increasing spiked concentrations of NFN (curves b−d) confirmed the absence of NFN in the unspiked urine sample. The recovery results found in the range of 97.75−99.60% of NFN in urine (Table S1) with a % RSD under 2.0% validated the

https://doi.org/10.1021/acsomega.3c00805
ACS Omega 2023, 8, 25758−25765

Table 2. Comparison of Several Electrochemical Methods for NFN Determination

substrate	modifier	method	dynamic range (μM)	LoD (μM)	ref
GCE	EPPGS	SWV	0.5−50.0	0.283	3
GCE	MWCNT-CPE/prGO-ANSA/Au	DPV	0.03−1.0 and 1.0−50.0	0.016	12
GCE	Ni/NiO/C/β-CD/RGO	DPV	0.4−80.0	0.01	14
GCE	MWCNT/Nafion	SWV	0.1−100.0	0.05	17
GCE	CuO/MWCNTs	DPV	1.0−47.7	0.321	18
GCE	poly(methyl red)	LSV	1.0−100.0	0.1	19
	pretreated boron-doped diamond electrode	SWV	0.016−12.5	0.004	26
GCE	poly(ANSA)	SWV	0.01−400.0	0.0041	this work

applicability of the developed method for the determination of NFN in human urine with a complex matrix.

3.7.1.2. Tablet Samples. The spike recovery experiment was also carried out in tablet samples by spiking the previously analyzed EAP and SSP brand tablet samples which showed the highest and least NFN content among the studied three brands with NFN standard solutions of 0.0, 40.0, and 80.0 μM (Figure S8). As shown in Table S2, spiked recovery results in the range of 98.35−101.2% confirmed the accuracy of the developed method and hence its applicability for the determination of NFN in tablet formulations. From this, it could be concluded that the low NFN content detected in the EAP brand tablet is not due to the low performance of the method but due to a lower NFN content than the labels.

3.7.2. Interference Study. The potential applicability of the method for determining NFN in the presence of particular potential interferents was investigated. The effect of selected potential interferents [ampicillin (AMP), chloroquine phosphate (CQP), and cloxacillin (CLOX)] was investigated at various levels (Figure S9) added to a 20.0 μM SSP brand NFN tablet sample. The claimed NFN level in the tablet sample was detected with an associated error under 2.13% (Table S3) even in the presence of different concentrations of AMP, CQP, and CLOX, showing the accuracy and selectivity of the method and hence validating its applicability for the determination of NFN in real samples.

3.8. Stability and Reproducibility Studies. The current response of the poly(ANSA)/GCE for 1.0 mM NFN in pH 7.5 PBS with an error of only 3.0% (% RSD) for five successive SWV measurements recorded at an interval of 2 h in a day (Figure S10A) and with an error of less than 3.2% for five SWV measurements in 20 days recorded at an interval of 4 days (Figure S10B) showed the stability of the modifier and hence the reproducibility of the results. In general, the precision, accuracy, selectivity, reproducibility of the results, and stability of the electrode modifier validated the developed method for the determination of NFN in various real samples.

3.9. Comparison of the Present Method with Previously Reported Methods. In terms of linear dynamic range, LoD, nature of the electrode substrate, and cost and availability of the electrode modifier, the performance of the proposed method was compared to those of previously released voltammetric methods for NFN measurement. Table 2 shows that the current method based on the poly(ANSA)/GCE, which just requires a simple electrode modification step, has the lowest detection limit and a relatively larger linear dynamic range than the other recently reported works.

4. CONCLUSIONS

In this work, the electrochemical behavior of NFN, the effects of scan rates, and the pH of the solution on the peak current and peak potential of NFN at the surface of the modified electrode were studied with CV. An irreversible oxidation peak at the poly(ANSA)/GCE with a much reduced overpotential fivefold than at the GCE, indicated an excellent catalytic role for the modifier toward NFN.

A better coefficient of determination (R^2) for the relationship between peak current and the square root of the scan rate indicated that the oxidation of NFN at the poly(ANSA)/GCE was predominantly diffusion-controlled. A SWV method based on the poly(ANSA)/GCE was used to quantify NFN in the complex matrix of three brands of tablet formulation and human urine samples. Under optimized SWV method parameters and solution pH (7.5), an excellent coefficient of determination (R^2) of 0.99911 for linear dependence of the oxidation peak current on the concentration in the range of 0.01−400.0 μM, low detection and quantification limit values of 0.41 and 1.36 nM, respectively, and excellent spike and interference recovery results validated the applicability of the method for the determination of NFN in tablet and urine samples. The sensor has shown good selectivity in the presence of AMP, CQP, and CLOX and repeatability and reproducibility with RSD less than 5%, which makes the method is a promising technique for the determination of NFN in tablet and urine samples.

■ ASSOCIATED CONTENT

Supporting Information

The Supporting Information is available free of charge at https://pubs.acs.org/doi/10.1021/acsomega.3c00805.

Cyclic voltammograms of NFN at various potential window and number of polymerization scan cycles, cyclic voltammograms of the sensors, supporting electrolytes, peak current vs scan rate and square root of scan rate, SWV optimized parameters, SWV of NFN in tablets, recovery study in real samples (urine and tablets), interference study summary, and stability of the sensor (PDF).

■ AUTHOR INFORMATION

Corresponding Authors

Adane Kassa − *Department of Chemistry, College of Natural and Computational Sciences, Debre Markos University, Debre Markos 269, Ethiopia; Department of Chemistry, College of Science, Bahir Dar University, Ethipia 79, Ethiopia*; Email: adanekss97@gmail.com

Molla Tefera − *Department of Chemistry, College of Science, University of Gondar, Gondar 196, Ethiopia*; orcid.org/0000-0003-4469-5388; Phone: +251-913141619; Email: mollatef2001@gmail.com, molla.tefera@uog.edu.et

https://doi.org/10.1021/acsomega.3c00805
ACS Omega 2023, 8, 25758−25765

Authors

Ameha Debalkie − *Department of Chemistry, College of Science, University of Gondar, Gondar 196, Ethiopia*

Atnafu Guadie − *Department of Chemistry, College of Science, University of Gondar, Gondar 196, Ethiopia*

Complete contact information is available at: https://pubs.acs.org/10.1021/acsomega.3c00805

Author Contributions

All authors have given approval to the final version of the manuscript and the authors declare no competing financial interest.

Notes

The authors declare no competing financial interest.

■ ACKNOWLEDGMENTS

The authors thank Addis Pharmaceutical Factory (APF), the Ethiopian Food and Drug Administration Authority (EFDA), and the College of Science at Bahir Dar University for providing standards and access to laboratory resources. We also thank the University of Gondar for financial support.

■ REFERENCES

(1) Verma, T.; Aggarwal, A.; Singh, S.; Sharma, S.; Sarma, S. J. Current challenges and advancements towards discovery and resistance of antibiotics. *J. Mol. Struct.* **2022**, *1248*, 131380.

(2) Yanat, B.; Rodríguez-Martínez, J. M.; Touati, A. Plasmid-mediated quinolone resistance in Enterobacteriaceae: a systematic review with a focus on Mediterranean countries. *Eur. J. Clin. Microbiol. Infect. Dis.* **2017**, *36*, 421−435.

(3) Fang, L.; Miao, Y.; Wei, D.; Zhang, Y.; Zhou, Y. Efficient removal of norfloxacin in water using magnetic molecularly imprinted polymer. *Chemosphere* **2021**, *262*, 128032.

(4) Liu, J.; Liu, W.; Zhou, S. N.; Wang, D. M.; Gong, Z. J.; Fan, M. K. Free-Standing Membrane Liquid State Platform for SERS-Based Determination of Norfloxacin in Environmental Samples. *J. Anal. Test.* **2021**, *5*, 217−224.

(5) Yadav, A. K.; Dhiman, T. K.; Lakshmi, G. B. V. S.; Berlina, A. N.; Solanki, P. R. A highly sensitive label-free amperometric biosensor for norfloxacin detection based on chitosan-yttria nanocomposite. *Int. J. Biol. Macromol.* **2020**, *151*, 566−575.

(6) Huang, Q.; Fang, C.; Muhammad, M.; Yao, G. Assessment of norfloxacin degradation induced by plasma-produced ozone using surface-enhanced Raman spectroscopy. *Chemosphere* **2020**, *238*, 124618.

(7) Keskar, M.; Jugade, R. Spectrophotometric determination of norfloxacin in pharmaceutical formulations based on charge transfer reaction with quinalizarin. *Anal. Chem. Lett.* **2015**, *5*, 319−328.

(8) da Cunha Xavier, J.; de Almeida-Neto, F. W. Q.; Rocha, J. E.; Freitas, T. S.; Freitas, P. R.; de Araújo, A. C.; da Silva, P. T.; Nogueira, C. E.; Bandeira, P. N.; Marinho, M. M.; et al. Spectroscopic analysis by NMR, FT-Raman, ATR-FTIR, and UV-Vis, evaluation of antimicrobial activity, and in silico studies of chalcones derived from 2-hydroxyacetophenone. *J. Mol. Struct.* **2021**, *1241*, 130647.

(9) Qin, D.; Zhao, M.; Wang, J.; Lian, Z. Selective extraction and detection of norfloxacin from marine sediment and seawater samples using molecularly imprinted silica sorbents coupled with HPLC. *Mar. Pollut. Bull.* **2020**, *150*, 110677.

(10) Wang, C.; Yu, G.; Chen, H.; Wang, J. Degradation of norfloxacin by hydroxylamine enhanced fenton system: Kinetics, mechanism and degradation pathway. *Chemosphere* **2021**, *270*, 129408.

(11) Liu, J.; Ma, L.; Zhao, T.; Yang, K.; Shi, H.; Kang, W.; Ma, L. Investigation on Ruthenium (II) Bipyridine/Ag III Complexes Chemiluminescence System and Its Application for Sensitive Norfloxacin and Ofloxacin Detection. *J. Braz. Chem. Soc.* **2019**, *30*, 867−872.

(12) Liu, Z.; Jin, M.; Cao, J.; Wang, J.; Wang, X.; Zhou, G.; van den Berg, A.; Shui, L. High-sensitive electrochemical sensor for determination of Norfloxacin and its metabolism using MWCNT-CPE/pRGO-ANSA/Au. *Sens. Actuators, B* **2018**, *257*, 1065−1075.

(13) Kassa, A.; Abebe, A.; Amare, M. Synthesis, characterization, and electropolymerization of a novel Cu (II) complex based on 1, 10-phenanthroline for electrochemical determination of amoxicillin in pharmaceutical tablet formulations. *Electrochim. Acta* **2021**, *384*, 138402−138415.

(14) Cui, X.; Cao, D.; Djellabi, R.; Qiao, M.; Wang, Y.; Zhao, S.; Mao, R.; Gong, Y.; Zhao, X.; Yang, B. Enhancement of Ni/NiO/graphitized carbon and β-Cyclodextrin/reduced graphene oxide for the electrochemical detection of norfloxacin in water sample. *J. Electroanal. Chem.* **2019**, *851*, 113407.

(15) Khairy, M.; Mahmoud, B. G.; Banks, C. E. Simultaneous determination of codeine and its co-formulated drugs acetaminophen and caffeine by utilising cerium oxide nanoparticles modified screen-printed electrodes. *Sens. Actuators, B* **2018**, *259*, 142−154.

(16) Tang, T.; Zhou, M.; Lv, J.; Cheng, H.; Wang, H.; Qin, D.; Hu, G.; Liu, X. Sensitive and selective electrochemical determination of uric acid in urine based on ultrasmall iron oxide nanoparticles decorated urchin-like nitrogen-doped carbon. *Colloids Surf., B* **2022**, *216*, 112538.

(17) Huang, K.-J.; Liu, X.; Xie, W.-Z.; Yuan, H.-X. Electrochemical behavior and voltammetric determination of norfloxacin at glassy carbon electrode modified with multi walled carbon nanotubes/Nafion. *Colloids Surf., B* **2008**, *64*, 269−274.

(18) Devaraj, M.; Deivasigamani, R. K.; Jeyadevan, S. Enhancement of the electrochemical behavior of CuO nanoleaves on MWCNTs/GC composite film modified electrode for determination of norfloxacin. *Colloids Surf., B* **2013**, *102*, 554−561.

(19) Huang, K.-J.; Xu, C.-X.; Xie, W.-Z. Electrochemical behavior of norfloxacin and its determination at poly (methyl red) film coated glassy carbon electrode. *Bull. Korean Chem. Soc.* **2008**, *29*, 988−992.

(20) Jayaprakash, G. K.; Kumara Swamy, B.; Rajendrachari, S.; Sharma, S. C.; Flores-Moreno, R. Dual descriptor analysis of cetylpyridinium modified carbon paste electrodes for ascorbic acid sensing applications. *J. Mol. Liq.* **2021**, *334*, 116348.

(21) Magar, H. S.; Hassan, R. Y.; Mulchandani, A. Electrochemical impedance spectroscopy (EIS): Principles, construction, and biosensing applications. *Sensors* **2021**, *21*, 6578.

(22) Gashu, M.; Aragaw, B. A.; Tefera, M. Voltammetric Determination of Oxytetracycline in Milk and Pharmaceuticals samples using Polyurea Modified Glassy Carbon Electrode. *J Food Compost Anal.* **2023**, *117*, 105128.

(23) Tefera, M.; Tessema, M.; Admassie, S.; Iwuoha, E. I.; Waryo, T. T.; Baker, P. G. Electrochemical determination of phenothrin in fruit juices at graphene oxide-polypyrrole modified glassy carbon electrode. *Sens. Bio-Sens. Res* **2018**, *21*, 27−34.

(24) Laviron, E. General expression of the linear potential sweep voltammogram in the case of diffusionless electrochemical systems. *J. Electroanal. Chem. Interfacial Electrochem.* **1979**, *101*, 19−28.

(25) Kassa, A.; Amare, M.; Benor, A.; Tigineh, G. T.; Beyene, Y.; Tefera, M.; Abebe, A. Potentiodynamic poly (resorcinol)-modified glassy carbon electrode as a voltammetric sensor for determining cephalexin and cefadroxil simultaneously in pharmaceutical formulation and biological fluid samples. *ACS Omega* **2022**, *7*, 34599−34607.

(26) Karahan, F.; Başı, Z.; Keskin, E.; Pınar, P. T.; Yardım, Y.; Şentürk, Z. Electrochemical Determination of Fluoroquinolone Antibiotic Norfloxacin in the Presence of Anionic Surfactant Using the Anodically Pretreated Boron-Doped Diamond Electrode. *ChemistrySelect* **2020**, *5*, 12862−12868.